ENTRAINMENT AND EVAPORATION OF DROPS IN THE LAMINAR PART OF A TWO-DIMENSIONAL DEVELOPING MIXING LAYER

F. Fichot, J. Bellan* and K. Harstad
Jet Propulsion Laboratory
California Institute of Technology
Pasadena. CA 91109

Word count:

text	3234	(14 words/line x 22 lines/page x 10.5 pages of text only)
equations	294	(21 x 14)
figures	2200	(2X 200 + 6 X 300)
total	5728	

Prefer oral presentation and publication' in the Proceedings.
The paper can be classified under Numerical Modeling (B) and the subject categories are 2.7 and 7.3.

" Corresponding author.
Phone (818) 354-6959
FAX (818) 393-1633
email - up to 1/1/94 FLORIAN @CALTECH.EDU
· after 1/1/94 J. BELLAN.JPL.354.GOV

ABSTRACT'

A formulation has been developed which combines the simplicity of an experimentally-derived well-established correlation for describing the development of a mixing layer, and a rigorous approach for the description of the dynamics and evaporation of dense or dilute clusters of drops in large coherent vortices.

An extensive parametric study has been performed by varying the radius of the drops in the drop-laden stream both for high and low air/fuel mass ratio, as well as for constant initial drop number density, but at varying air/fuel mass ratio. The air/fuel mass ratio has also been varied at fixed drop radius in the drop-laden stream. Additional parameters independently varied were the temperature of the hot air stream, its velocity and the velocity ratio between the two streams.

The results show that it is possible to optimize the relative number of drops (with respect the initial value) entrained into the coherent vortices of the mixing layer by using the the velocity ratio as control parameter. The eventual liquid mass entrained in the cluster is an increasing function of the drop radius in the drop-carrying stream for typical drop number densities in sprays. The mass fraction of the evaporated fuel in the clusters can be optimized by using the velocity of the hot air stream as control parameter.

It is also shown that, in agreement with existing observations, the average drop radius may increase with axial distance from the mixing layer inception point, and the reasons for this are explained.

INTRODUCTION

Mixing layers are an inherent feature of many particle-laden flows. They occur whenever a particle-laden flow travels with a velocity different from that of the flow around it. In fuel sprays injected in combustion chambers, the mixing layer at the edge of the spray has the important function of transferring heat from the ambient to the spray. During this process, momentum transfer and mass transfer occur as, well.

Hernan and Jimenez[1] showed that most of the momentum transfer in a mixing layer occurs before paring of the large-scale coherent vortices which are instrumental in both momentum transfer and drop dispersion. Drop dispersion in shear layers, mixing layers wakes and jets have been extensively studied for small particle-loading by mass[2-6], for small particle-loading by volume[2-6], or for large particle-loading by mass in the case of particles made of a heavy material such as glass[7]. In these situations, the interaction between flow and particles is limited to the flow influencing the dynamics of the particles. The effect of the particles on the flow is minimal (except when the particle loading is very large by mass) and the interaction between the particles is negligible. No equivalent studies exist in situations when the particle-number-density is very large to the point that the particles affect the dynamics of the flow, and that there is substantial particle thermodynamic interactions affecting the heating and evaporation of particles. The reason for the lack of investigations in these more complicated situations is the difficulty of performing experimental measurements in the high particle-number-density regime, and the difficulty of modeling the two-way coupling between particles and flow as well as the multiparticle thermodynamic interactions.

The modeling approach described in this manuscript shows that it is possible to achieve a qualitative understanding of high-number-density particle-laden mixing layers by

using a combination of rigorous analysis and well-established experimental correlations.

PHYSICAL CONFIGURATION AND FORMULATION

Figure 1 shows the physical configuration modeled here. A two-dimensional (2D) mixing layer is established between two streams separated by a splitter plate: a hot air stream characterized by temperature T_1, density ρ_1 and velocity U_1, and a drop-laden stream at a lower temperature and higher velocity. The drop number density, temperature, density and velocity of the drops are n_2, T_{2d}, ρ_l and U_{2d} and the equivalent quantities for the carrying flow are T_{2g}, ρ_{2g} and U_{2g}. According to the results of Brown and Roshko[8] and Roshko[9], the mixing layer is characterized by large coherent vortices convecting downstream. Ho and his coworkers[10,11] have observed that a particle-free mixing layer remains laminar for an extended length before the appearance of small scale turbulent structures and that their inception point is determined from the initial Strouhal number, Str^o, and the initial vorti city thickness, δ^o. The present model pertains to the laminar part of the mixing layer.

The large coherent vortices of the mixing layer convect at velocity UC with respect to the splitter plate trailing edge, and it is assumed that, according to observations, they can be portrayed in 2D by circles[1] whose diameter grows linearly with abscissa[12]. The entrainment rate from the hot air stream is $\dot{V}_1$, whereas the gas and drop entrainment rate from the second stream are $\dot{V}_{2g}$ and $\dot{V}_{2d}$. For particle-free, 2D, fully developed, spatially growing, subsonic shear layers, the entrainment rates from the two streams has been correlated[1 2] from an extensive number of experiments to be

$$E_v = \dot{V}_2 / \dot{V}_1 = f^{1/2} [1 + 0.33 (1 - s) (1 + f^{1/2}) / (1 + sf^{1/2}] \qquad (1)$$

where $s = U_2/U_1$ and $f = \rho_2/\rho_1$. The same correlation is assumed to be valid in the present situation except that $s = \bar{U}_2/U_1$ and $f = \bar{\rho}_2/\rho_1$ where (-) represents an average over gas and

drops.

It is additionally assumed that the drops form a cluster similar to those observed in jets and sprays[7,13-15], that the cluster is monodisperse (the averaging is based upon liquid mass conservation and evaporation-rate continuity) and that the outer boundary of the cluster and vortex coincide being located the radial position R_{ou} ("out' stands for outer) from the center of the vortex. The vortex boundary is defined as the boundary of the volume containing the gas entrained into the vortex, so that if r is the radial coordinate from the cluster center, $U_{ou} = U_{gr,ou}$. Other assumptions are: the vortex has a constant outer tangential velocity; the radial and azimuthal velocity of drops and gas can be expressed as sums of irrotational and solid body motion[16]; the entrained gas angular momentum is distributed throughout the vortex and it is modeled as the sum of an irrotational motion and a solid body motion; and, the angular momentum of the entrained drops is neglected. The number of drops entrained in the vortex per second and unit vortex length is $\alpha_d \dot{V}_{2g} n_2$ where α_d depends upon the Stokes number, $St = \rho_l (2R^o_d)^2 |U_{2d} - UC| / (18\mu R_{ou})$, where R^o_d is the initial drop radius, and μ is the gas viscosity. Consistent with observations[5,6], $\alpha_d = 1$ if $St < 10^{-*}$ and $\alpha_d = O$ if $St > 10$. For $10^{-1} < St < 10$, here $\alpha_d = 0{,}5(1 - \mathrm{Log}_{10} St)$, so that a continuous function $\alpha_d (St)$ is obtained.

Averaging processes for the drop-carrying stream yield $\bar{\rho}_2 = (1 + \Phi^o) n_2 m^o_d$ where Φ^o is the initial air/fuel mass ratio in the stream, and m^o_d is the initial mass of a drop. If one defines $\bar{U}_2$ from $\bar{\rho}_2 (U_c - \bar{U}_2)^2 \equiv \rho_1 (U_1 - U_c)^2$ consistent with [12], then $\rho_1 (U_1 - U_c)^2 \equiv \bar{\rho}_2 (U_c - U_{2g})^2 + n_2 m^o_d (2U_c - U_{2g} - U_{2d}) (U_{2g} - U_{2d})$. Finally, an average outer tangential velocity of the gas is defined as $U_{g0,ou} = [\rho_1 \dot{V}_1 (U_1 - U_c) + \rho_{2g} \dot{V}_{2g} (U_{2g} - U_c)] / (\rho_1 \dot{V}_1 + \rho_{2g} \dot{V}_{2g})$.

The conservation equations are as follows:

1) continuity of the evaporation rate

$$dN_c/dt + (d\bar{R}_d/dt)\, N_c/\bar{R}_d = \alpha_d \dot{V}_{2g} n_2 R_d^o/\bar{R}_d - 2\pi R_{ou} n_c \max(0; u_{d,ou} - u_{ou}) - N_c \dot{m}_{ev}/(3m_d) \quad (2)$$

where N_c is the number of drops and n_c is the drop number density in the cluster, $n_c = N_c/[\pi(R_{ou}^2 - R_{in}^2)]$ where "in" identifies the inner cluster radius, $\bar{R}_d$ is the averaged drop radius in the cluster and the drop evaporation rate, $\dot{m}_{ev}$, is taken proportional to Rd. The second term in the right hand side (RHS) accounts for drops lost from the cluster through centrifugation.

2) conservation of liquid mass

$$dN_c/dt + (d\bar{R}_d/dt)\, 3N_c/\bar{R}_d = \alpha_d \dot{V}_{2g} n_2 (R_d^o/\bar{R}_d)^3 - 2\pi R_{ou} n_c \max(0; u_{d,ou} - u_{ou}) - N_c \dot{m}_{ev}/m_d \quad (3)$$

3) conservation of gas mass, m_g

$$dm_g/dt = -(dN_c/dt)(m_g + m_d)/N_c + \rho_1 \dot{V}_1 (1 + C_{TM})/N_c - 2\pi R_{in} \rho_g (u_{d,in} - u_{g,in})/N_c + \dot{m}_{ev}$$

$$- 2\pi n_c m_d \max(0; u_{d,ou} - u_{ou})/N_c + n_2 m_d^o E_v \dot{V}_1/N_c \quad (4)$$

where $C_{TM} = E_v (T_1 / T_{2g}) / [\Phi^o/(\Phi^o + \rho_{2g}/\rho_1)]$.

4) conservation of the air mass, m_a

$$N_c dm_a/dt = -(dN_c/dt)\, m_a + \rho_1 \dot{V}_1 [1 + C_{TM}(1 - Y_{FV}^o)] - 2\pi R_{in} \rho_g (u_{d,in} - u_{g,in})\, Y_{a,i} + D_{a,ou} N_c \quad (5)$$

Where Y^o_{FV} is the initial mass fraction of vapor fuel, $Y_{a,i}$ is the mass fraction of air in the interstitial cluster region defined by the space between the spheres of influence around each drop, and $D_{a,ou}$ accounts for air mass diffusion at the vortex boundary [16]. The sphere of influence for each drop is defined[16] as centered at the drop center and having for radius the half distance between the centers of two adjacent drops.

5) conservation of gas angular momentum

$$\rho_g [\partial u_{g\theta}/\partial t + u_{g\theta} (\partial u_{g\theta}/\partial r) + u_{gr}\, u_{g\theta}/r] = F_{g\theta} + \frac{\gamma_1}{r} + \gamma_2 r \qquad (6)$$

where

$$F_{g\theta} = n_c (\dot{m}_{ev} + 0.5\rho_g A_d \mathrm{CD} |\vec{U}_s|) (U_{d\theta} - U_{g\theta}) \qquad (7)$$

$$\int_0^{R_{ou}} (\gamma_1/r + \gamma_{2r})\, 2\pi r dr = \rho_1 \dot{V}_1 (1 + C_{TM})\, U_{g\theta,ou} \qquad (8)$$

$$\partial U_{g\theta,ou} / \partial t = 0 \qquad (9)$$

In Eqs.6-9, $F_{g\theta}$ is the drag force, U_s is the slip velocity, A_d is the drop surface area, C_D is the drag coefficient, γ_1 is the irrotational motion of the gas and γ_2 is the solid body rotation of the gas.

6) conservation of mass in the inner vortex core devoid of drops

$$R_{in} u_{gr,in} = -0.5 R_{in}^2 (d\ln\rho_g/dt) + \rho_1 \dot{V}_1 (1+C_{TM}) R_{in}^2 / (2\pi R_{ou}^2 \rho_g) \qquad (10)$$

7) global conservation of total enthalpy

$$dH_g/dt = (H_g + 0.5 m_d \langle u_d^2 \rangle_i + H_d)(dN_c/dt)/N_c + \dot{m}_{ev}\{C_{pfv} T_{gs} - C_p (T_{gi} - T_{gs})$$

$$/ [\exp[\beta (Z_s - Z_i)_1 - 1]\} + 2\pi R_{in} \rho_g C_{pg} T_{gi} (u_{d,in} - u_{g,in})/N_c$$

$$+ \rho_1 \dot{V}_1 T_1 (C_{p1} + C_{p2} C_{TM})/N_c - 0.5 d[m_d \langle u_d^2 \rangle_r]/dt$$

$$+ n_2 m_d^o C_{p1} T_{2_d} V_1 N_c - 2\pi R_{ou} n_c H_d \max(0; u_{d,ou} - u_{g,ou}) + D_{H_{g,ou}} \qquad (11)$$

In Eq. 11 the terms in the RHS represent respectively: the changes due to the number of drops variation; a source due to evaporation; a sink due to gas lost to the vortex core; a source due to gas entrainment from both streams; a sink due to the time change in the drops

kinetic energy; asourcedue to drops entrainment from the drop-laden stream; asink due to loss of drops which are centrifuged out from the cluster; and diffusion of heat from the outer gas phase at the vortex boundary[16]. H_g is the gas enthalpy, H_d is the enthalpy of a drop, $H_d = m_d C_{pl} 4\pi \int_0^{R_d} T_d(r) r^2 dr$ and C_p is the heat capacity at constant pressure. The averaging symbol $< >$ is over all drops either in the interstitial space (subscript i), or in the radial direction (subscript r). Quantities β and $Z(r_d)$ have been calculated previously[17,18] together with the solution of the diffusion equations inside the sphere of influence of each drop. The radial coordinate inside the sphere of influence is r_d, and Z_s and Z_i are the values at the drop surface and at the edge of the sphere of influence respectively. Here $\beta = -\dot{m}_{ev}/(4\pi R^o_d)$ and $Z(r_d) = (\theta^{ou}_g)^{0.65} \int_0^{R_i} dr_d/(r^2_d \theta^{ou}_g)^{0.65}$, where $\theta_g = C_{pg} T_g / L_{bn}$ with L_{bn} being the latent heat of evaporation, and R_i being the radius of the sphere of influence.

The radial gas momentum equations and the momentum equations for the drops have been derived previously[16].

INITIAL CONDITIONS

It is assumed that the cluster is initially a small ring defined by R^o_{ou} and R^o_{in}, and thus the initial Lagrangian coordinate defining the cluster position, X^o_c, is non null. An extrapolation of the linear growth rate[12] is used to find the time, $\hat{t}$, at which R^o_{ou} is reached, and thus $X^o_c = u_c \hat{t}$ is found.

Initial dependent variables in the cluster have the same value as those in the drop-carrying stream so that $\Phi^o_c = \Phi^o_2$, $T^o_{gi} = T_{2g}$, $Y^o_{ji} = Y_{2j}$, where "j" denotes a species.

The calculations are stopped at the onset of small scale turbulence defined by XT = 4 (s + 1) L"/(s - 1) where Lo is the initial instability wavelength and $Str^o = \delta^o/L^o$.

DISCUSSION OF RESULTS

Ail calculations were performed for n-decane for which Φ^o_{stoich} = 15.7. Nominal

properties for n-decane were listed elsewhere[19]. Physical intuition indicates that competition between $\Re_1$ = (evaporation rate/entrainment rate) and $\Re_2$ = (drop ejection rate/entrainment rate) determines the drop size in the cluster. Simple, but tedious manipulations show that the residual drop radius decreases with time if $\Re_1 > 1$, and increases with time if $\Re_1 < 1$, independently of $\Re_2$. However if $\Re_2 > 1$, the liquid mass in the cluster decreases, and since $\bar{R}_d/R^o_d < 1$, NC decreases, whereas if $\Re_2 < 1$ the liquid mass in the cluster increases. For most situations analyzed here $\Re_1 > 1$ and $\Re_2 < 1$ initially.

A baseline calculation was performed for $U_1 \simeq$ lm/see, $U_{2d} = U_{2g}$ = 10m/see, R^o_d = 15μ, Φ^o = 1.5, T = lOOOK, T_{2d} = 350K and T_{2g} = 370K. The results show that three stages can be observed in the transient behavior of the mixing layer, but that these three stages are not necessarily separated. First, entrainment of hot air produces a decrease in the liquid/gas mass ratio, an increase in T_{gi} and a decrease in n_c due to gas expansion. Evaporation becomes important when T_{gi} and N_c increase, resulting in an approximately constant liquid/gas mass ratio and a decrease in n_c. Finally, R_d, T_{gi} and $Y_{FV,i}$ reach asymptotic values.

Parametric studies performed by varying R^o_d showed that quantitative behavior is different when Φ^o = 5 and Φ^o = 0.5. It should be realized that E_v = 1.25 when Φ^o = 5 and E_v = 2 when Φ^o = 0.5 because E_v depends upon Φ^o through $\tilde{\rho}_2$. Figures 2 and 3 show respectively T_{gi} and $Y_{FV,i}$ versus the Lagrangi an coordinate for various R^o_d' s for the two values of Φ^o. For initially higher mass and volume loading (and a larger E_v), evaporation is greatly delayed because of the higher drop number density. This explains the larger T_{gi} during the initial phase and the much smaller T_{gi} during the latter phase, after the drops have heated up and removed a substantial amount of heat from the gas (since n_c is larger). Once the drops are hot, evaporation becomes important and the decrease in T_{gi} corresponds

to a simultaneous increase in $Y_{FV,i}$. Smaller drops heat faster because of their smaller size. At fixed Φ^o, as R^o_d is smaller and thus n_2 (and n_c) is larger, the heat sink represented by the drops is larger, and thus the reduction in T_{gi} is larger.

A similar study was performed by varying R^o_d, but now n_2 was kept constant while Φ^o varied, and E_v increased from 1.14 for $R^o_d = 5\mu$ to 2.49 for $R"_d = 30\mu$. When Rod is smaller and n_2 is kept constant, the liquid mass is smaller and thus the drop-carrying stream (and the cluster) is more dilute. These more dilute clusters heat up faster, and their $\bar{R}_d/R^o_d$ decreases faster as the relative number of drops (with respect to $N"_c$) entrained is smaller. As a result, for these dilute clusters, $Y_{FV,i}$ is at most 10^{-2}. Figure 4 shows both that $\bar{R}_d/R^o_d$ stays larger with increasing $R"_d$ and that the drop number density peaks higher with increasing $R"_d$. Thus the eventual maximum liquid mass in the cluster is an increasing function of R^o_d at fixed n_2, U_1 and velocity ratio. The result is not necessarily obvious since larger drops are heavier and thus more difficult to entrain. Mathematically this is shown by the fact that fors > 1, E_v is a nonmonotonic function of Φ^o through Eq.1 and the definition of ρ_2. In the range of Φ^o (and thus $R"_d$ since n_2 is fixed) investigated here, E_v is an increasing function of Φ^o, thus explaining the results. It is expected that for larger drops and thus smaller Φ^o's, a maximum will be reached for the liquid mass entrained. Calculations proving this point are not shown because for these very large values of Rod, the eventual value of n_c is unrealistically large compared to spray observations.

Parametric studies performed by varying T_1 from 400K to 1300K (and accordingly E_v from 0.9 to 1.72) show that the relative number of drops entrained is insensitive to T_1 above 800K, whereas the value is much smaller for 400K. Since p = 1atm, a low T_1 implies a large ρ_1, and thus a smallers which hinders entrainment of particles. Since the results show that the residual drop radius is a decreasing function of T_1, whereas the drop number density

is an increasing function of T_1, the liquid mass entrained seems to be constant, except perhaps for T_1 = 400K, in agreement with the indications from the relative number of drops.

Figures 5 and 6 document in detail the influence of Φ^o upon the cluster behavior. Heating and evaporation dominate the initial regime, whereas drop entrainment dominates the final regime. The initial regime is itself composed of two distinct subregimes. The first subregime is characterized by entrainment of hot air, thus increasing T_{gi}, by drop centrifugation inside the vortex and cluster volume increase, thereby decreasing n_c, and by drop evaporation, thereby decreasing $\bar{R}_d$. For smaller Φ^o's, drop heating is slower and thus T_{gi} stays larger longer. The second subregime, starting around XC = 0.5cm, is characterized by an increase in drop entrainment from the drop-laden stream, as evidenced by the increase in the liquid-gas mass ratio, the relative number of drops and n_c; the result is a slower T_{gi} increase for small Φ^o's, and the formation of a plateau for larger Φ^o's corresponding to cooling of the gas phase due to drop heating. During this initial regime $\bar{R}_d$ decreases, resulting in only a moderate increase in $Y_{FV,i}$ because NC is still relatively low. The final regime initiates around XC = 1 cm and is characterized by a large increase in NC, resulting in an increase in the liquid-gas mass ratio and n_c (since the cluster volume increases only moderately). Heat transfer to a larger number of drops reduces T_{gi} substantially, and $Y_{FV,i}$ increases considerably. For smaller Φ^o's (i.e. larger n_2) there is a larger reduction in T_{gi} and increase in $Y_{FV,i}$. Despite evaporation, $\bar{R}_d$ increase because $\Re_1 < 1$. Lund et.al.[20] have indeed observed that the Sauter Mean Diameter can increase with axial position in a spray. The present results show the reasons for this observation. Consistent with this explanation, $\bar{R}_d$ increases most and the relative drop number increases least for the smaller Φ^o. As Φ^o is large and the drop-laden stream is dilute, entrainment of drops is not sufficient to increase $\bar{R}_d$, and instead $\bar{R}_d$ continues to decrease. For large Φ^o it is also easier to entrain the drops

(at fixed s), so that the relative drop number is maximum.

Results obtained by varying s parametrically are illustrated in Figs. 7 and 8. The initial and final regimes discussed above are here present as well, although they are not so clearly separated. Of special interest is the fact that past the very initial part of the calculation ($X_C > 0.25$ cm), T_{gi} and $Y_{FV,i}$ are respectively an increasing and a decreasing function of s. An exception is found for T_{gi} at very large values of s because of the optimization of the relative number of drops entrained as explained below. The relative number of drops entrained is a nonmonotonic function of s, just as it was shown to be a nonmonotonic function of R°_{d} at fixed s. The maximum relative number of drops occurs at s = 20, resulting in a reduction in T_{gi} since heat is removed by the drops from the gas phase. These results thus suggest that it is possible to optimize entrainment of drops from the mixing layer into the large coherent vortices by using the velocity ratio as control parameter. These findings complement existing results showing that drop dispersion in large coherent eddies is optimized at St = 1, a phenomenon which was called “the focusing effect"[6]. The present results show that additionally drop entrainment can be optimized by changings when Φ°, T_1, T_{2g}, T_{2d} and f are fixed.

Calculations were also performed by varying U_1 to be lm/see, 5m/see, 15m/see, 25m/sec and 50m/see, The results show that the relative drop number is an increasing function of U_1 (in agreement with the fact that E, is a decreasing function of s), but that $Y_{FV,i}$ is a nonmonotonic function of U_1, attaining a maximum at intermediate values (U_1 = 15m/sec).

The value of $Y_{FV,i}$ is determined by competition between evaporation, entrainment and volume expansion of the cluster. As U_1 increases, s decreases and E_v increases. As NC becomes larger, $\bar{R}_d$ increases to the point that $\dot{m}_{ev}$ decreases because of the larger time

necessary to heat the drops. Plots of $\overline{R}_d$ and T_{gi} show the largest increase in R_d and the largest reduction in T_{gi} for $U_1 = 25m/sec$, thereby supporting this interpretation.

SUMMARY AND CONCLUSIONS

A model of drop entrainment inamixing layer has been developed by combininga simplified formulation of the mixing layer based upon experimental correlations and a more rigorous formulation describing the dynamics and evaporation of dense or dilute clusters of drops in cylindrical, axisymmetric vortices.

Calculations' were performed by varying an extended number of parameters. The results show, in agreement with observations, that the average drop radius may increase with the distance from the inception of the mixing layer. Additionally, it is shown that in the range of drop number density values typical of sprays, it is possible to maximize the liquid mass entrained by using the drop radius as a parameter, and that it is possible to optimize the relative number of drops (with respect to the initial value) entrained into the large coherent vortices by using the velocity ratio between streams as parameter. The velocity of the hot air stream has been shown to be a parameter controlling the interstitial fuel vapor mass fraction.

ACKNOWLEDGMENTS

This work has been performed at the Jet Propulsion Laboratory under the sponsorship of the Societe Europeene de Propulsion (F.F.), and the U.S. Air Force Wright Patterson Laboratory (J.B. and K. H.) through an agreement with the National Aeronautics and Space Administration.

REFERENCES

1.Hernan, M.A., and Jimenez, J., J. Fluid Mech., 119: 323-345 (1982)

2.Lazaro, B.J. and Lasheras, J.C., J. Fluid Mech., 23:143-178 (1992)

3.Lazaro, B.J. and Lasheras, J.C., J. Fluid Mech., 235: 179-221 (1992)

4.Lazaro, B.J. and Lasheras, J.C., Phys. Fluids A., 1 (6): 1035-1044 (1989)

5. Crowe, C.T., Chung, J.N,. and Troutt, T.R., Prog. Energy Combust. Sci., 14: 171-194 (1988)

6.Crowe, C.T., Chung, J.N. and Troutt, T.R., Particulate Two Phase Flow, 1993 (Ed. M. Roco), Butterworth, Chpt. 18.

7.Longmire, F.K., and Eaton, J.K., J. Fluid Mech., 236:217-257 (1992)

8.Brown, G.L. and Roshko, A., J. Fluid Mech., 64(4): 775-816 (1974)

9.Roshko, A., AIAA Journal, 14 (10): 1349-1357 (1976)

10.Huang, L-S. and Ho, C-M., J. Fluid Mech., 210: 475-500 (1990)

11 .Zohar, Y. and Ho, C-M., "Dissipation Scale and the Control of Fine Scale Turbulence in a Mixing Layer, submitted to J. Fluid Mech.

12. Dimotakis, P., AIAA Journal, 24 (11): 1791-1796 (1986)

13. Mizutani, Y., Nakabe, K., Fuchihata, M., Akamatsu, F., Zaizen, M. and El-Emam, S. M., Atomization and Sprays, 3: 125-135 (1993)

14.McDonnel, V., Adachi, M. and Samuelsen, G.S., Combust. Sci. and Techn., 82: 225-248 (1992)

15. Rudoff, R. C., Brena de la Rosa, A., Sankar, S.V. and Bachalo, W.D., paper AIAA-89 -0052.

16. Bellan, J. and Harstad, K., 23rd Syrnp. (Int.) on Combustion, The Combustion Institute, Pittsburgh, 1990, pp. 1375-1381

17. Bellan, J., and Harstad, K., Int. J. Heat Mass Transfer, 31(8): 1655-1668 (1988)

18. Bellan, J. and Harstad, K., Combust. Flame, 79: 272-286 (1990)

19. Bellan, J. and Harstad, K., Int. J. Heat Mass Transfer, 30(1), 125-136(1987)

20. Lund, M.T., and Sojka, P. E., ILASS'93 Proc., 14-18, Worcester, Mass.

Figure Captions

Figure 1 Sketch of the two-dimensional mixing layer

Figure 2 Interstitial cluster gas temperature versus the vortex abscissa for $\Phi^o = 5$ (top) and for $\Phi^o = 0.5$ (bottom). Other parameters are U_1 = lm/see, $U_{2d} = U_{2g}$ = 10m/see, T_1 = lOOOK, T_{2g} = 370K, T_{2d} = 350K.

Figure 3 Interstitial fuel vapor mass fraction $(Y_{Fv,i})$ versus the vortex abscissa for $\Phi^o = 5$ (top) and for $\Phi^o = 0.5$ (bottom). Other parameters are U_1 = lm/see, $U_{2d} = U_{2g}$ = 10m/see, T_1 = lOOOK, T_{2g} = 370K, T_{2d} = 350K.

Figure 4 Residual drop radius $(\bar{R}_d/R^o_d)$ and drop number density (n_C) versus the vortex abscissa for fixed n_2 and varying R^o_d (and thus E_v). Other initial conditions are listed in Fig. 2 caption.

Figure 5 Drop number density in the cluster (n_c), relative drop number (with respect with $N"_C$) and drop residual radius $(\bar{R}_d/R^o_d)$ versus the vortex abscissa for various values of Φ^o. Other initial conditions are listed in Fig. 2 caption.

Figure 6 Interstitial cluster gas temperature (T_{gi}), fuel vapor mass fraction $(Y_{Fv,i})$, and liquid-gas mass ratio in the cluster versus the vortex abscissa for various values of Φ^o. Other initial conditions are listed in Fig. 2 caption.

Figure 7 Drop number density in the cluster(n C), relative drop number (with respect with $N"_C$) and drop residual radius $(\bar{R}_d/R^o_d)$ versus the vortex abscissa for various values ofs. Other initial conditions are listed in Fig. 2 caption.

Figure 8 Interstitial cluster gas temperature, fuel vapor mass fraction $(Y_{Fv,i})$, and liquid-gas mass ratio in the cluster versus the vortex abscissa for various values ofs. Other initial conditions are listed in Fig. 2 caption.

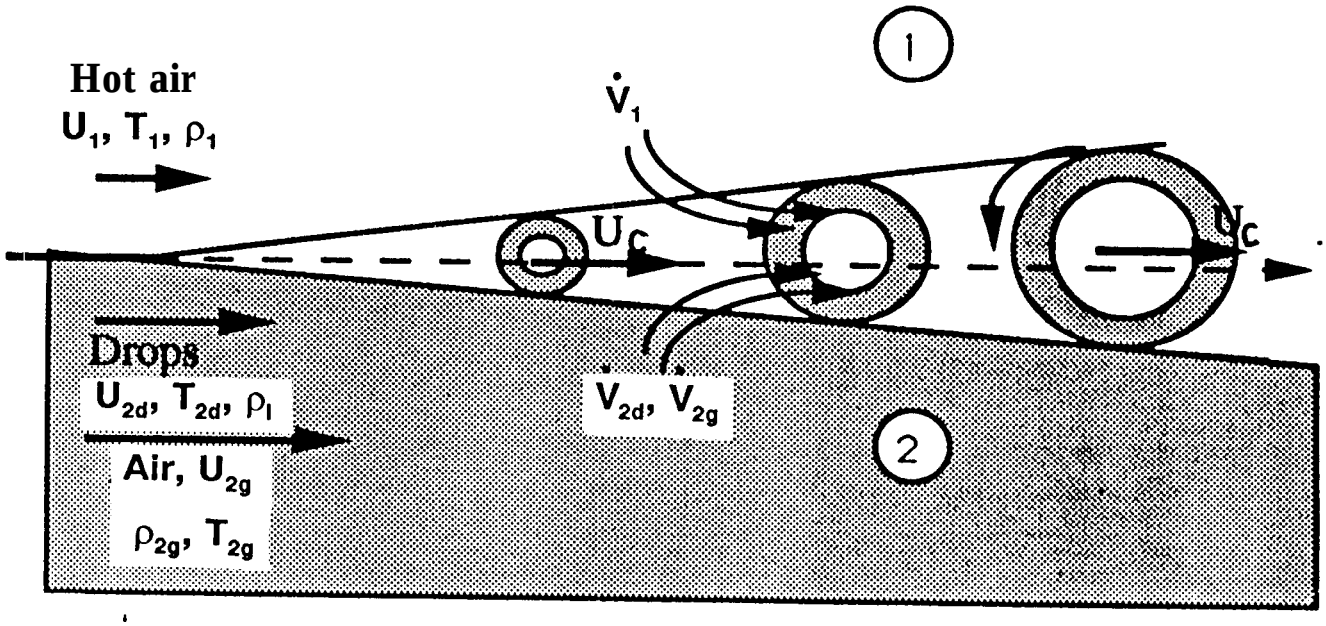
1
Hot air
U_1, T_1, ρ_1
$\dot{V}_1$
U_c
U_c
Drops
U_{2d}, T_{2d}, ρ_l
Air, U_{2g}
ρ_{2g}, T_{2g}
V_{2d}, V_{2g}
2

Fig 1

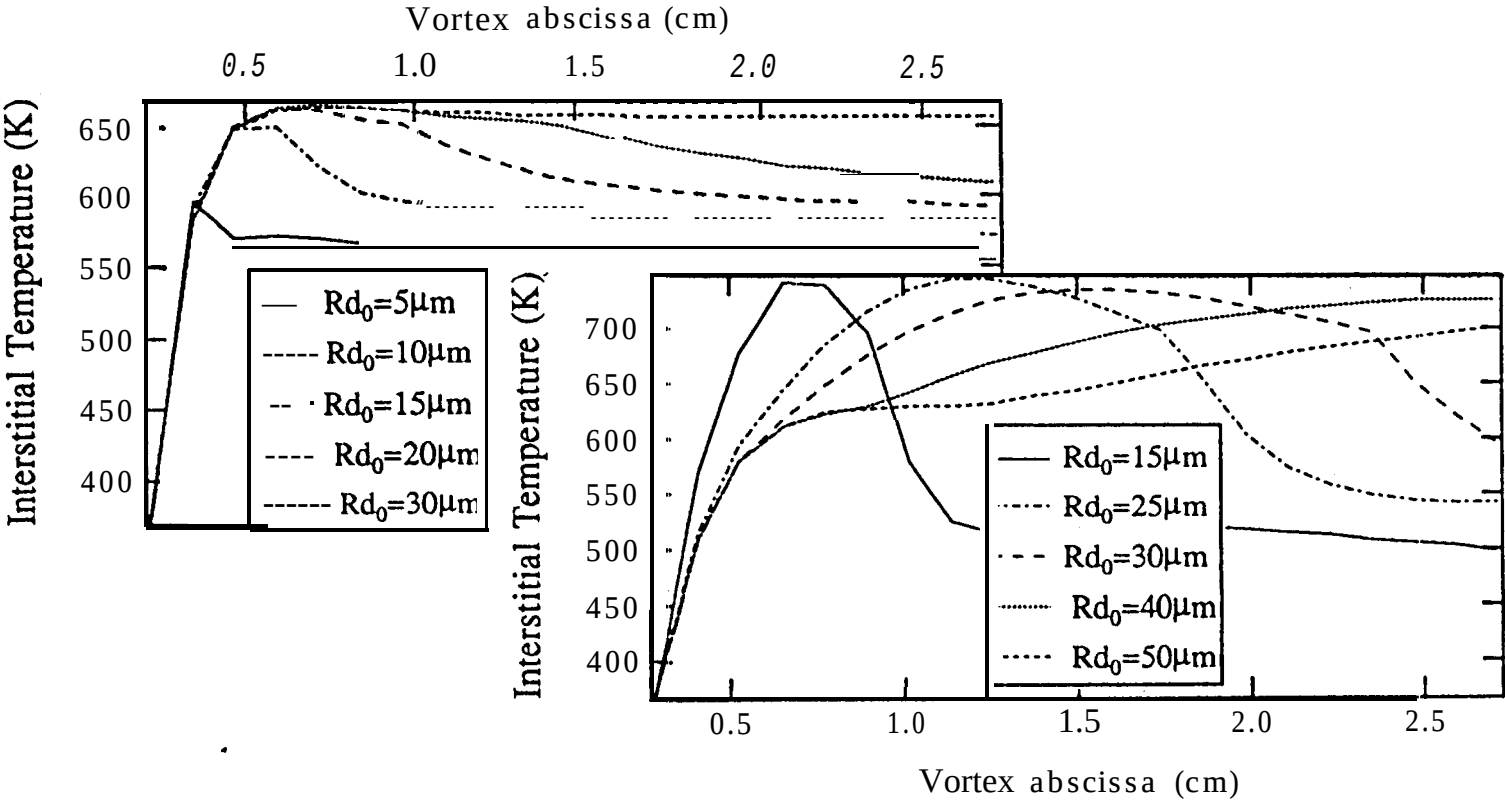
Vortex abscissa (cm)
0.5
1.0
1.5
2.0
2.5
Interstitial Temperature (K)
650
600
550
500
450
400
Rd0=5μm
Rd0=10μm
Rd0=15μm
Rd0=20μm
Rd0=30μm
Interstitial Temperature (K)
700
650
600
550
500
450
400
Rd0=15μm
Rd0=25μm
Rd0=30μm
Rd0=40μm
Rd0=50μm
0.5
1.0
1.5
2.0
2.5
Vortex abscissa (cm)

Fig 2

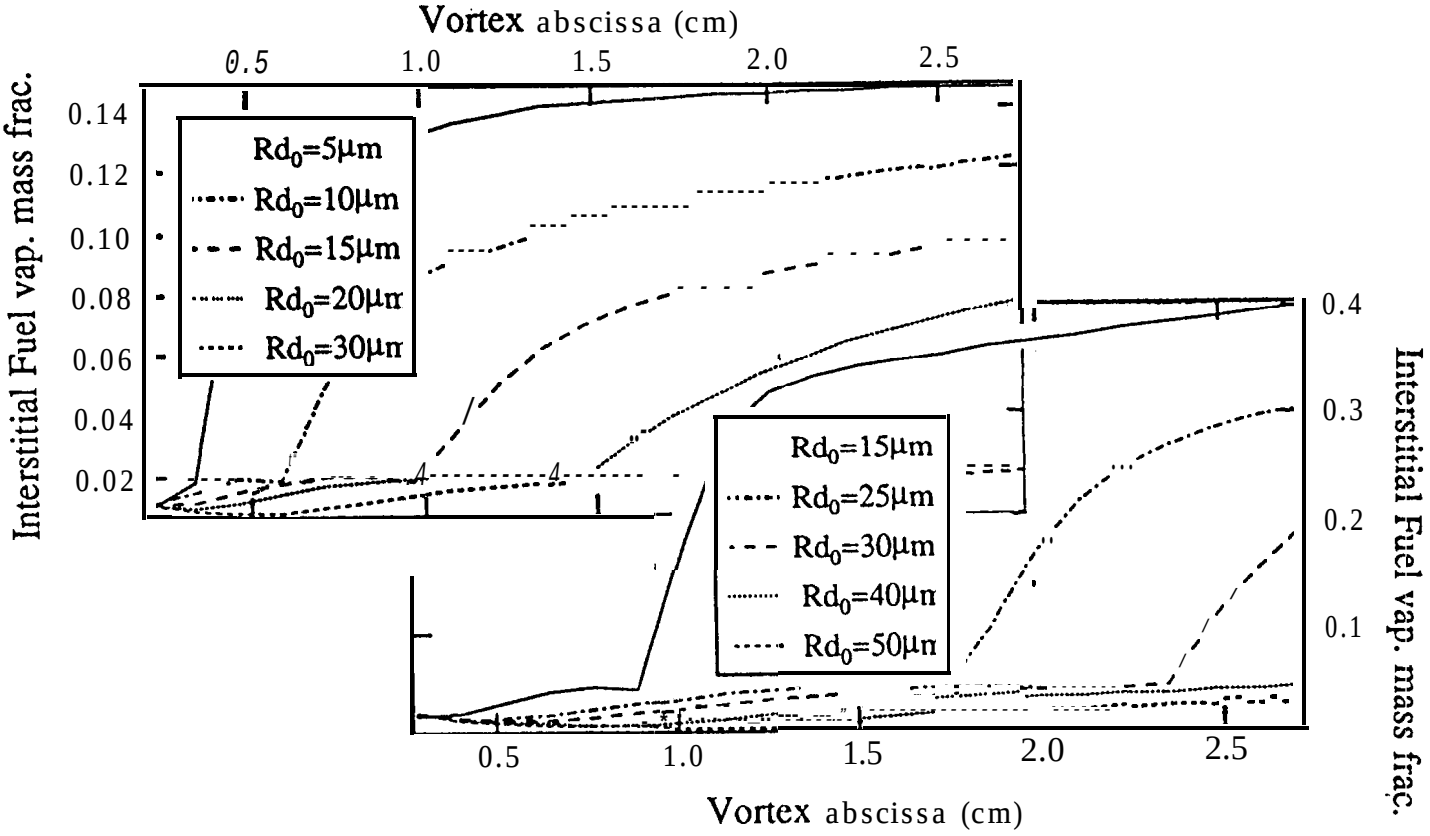
Vortex abscissa (cm)
0.5
1.0
1.5
2.0
2.5
Interstitial Fuel vap. mass frac.
0.14
0.12
0.10
0.08
0.06
0.04
0.02
Rd0=5μm
Rd0=10μm
Rd0=15μm
Rd0=20μm
Rd0=30μm
Rd0=15μm
Rd0=25μm
Rd0=30μm
Rd0=40μm
Rd0=50μm
0.4
0.3
0.2
0.1
Interstitial Fuel vap. mass frac.
0.5
1.0
1.5
2.0
2.5
Vortex abscissa (cm)

Fig 3

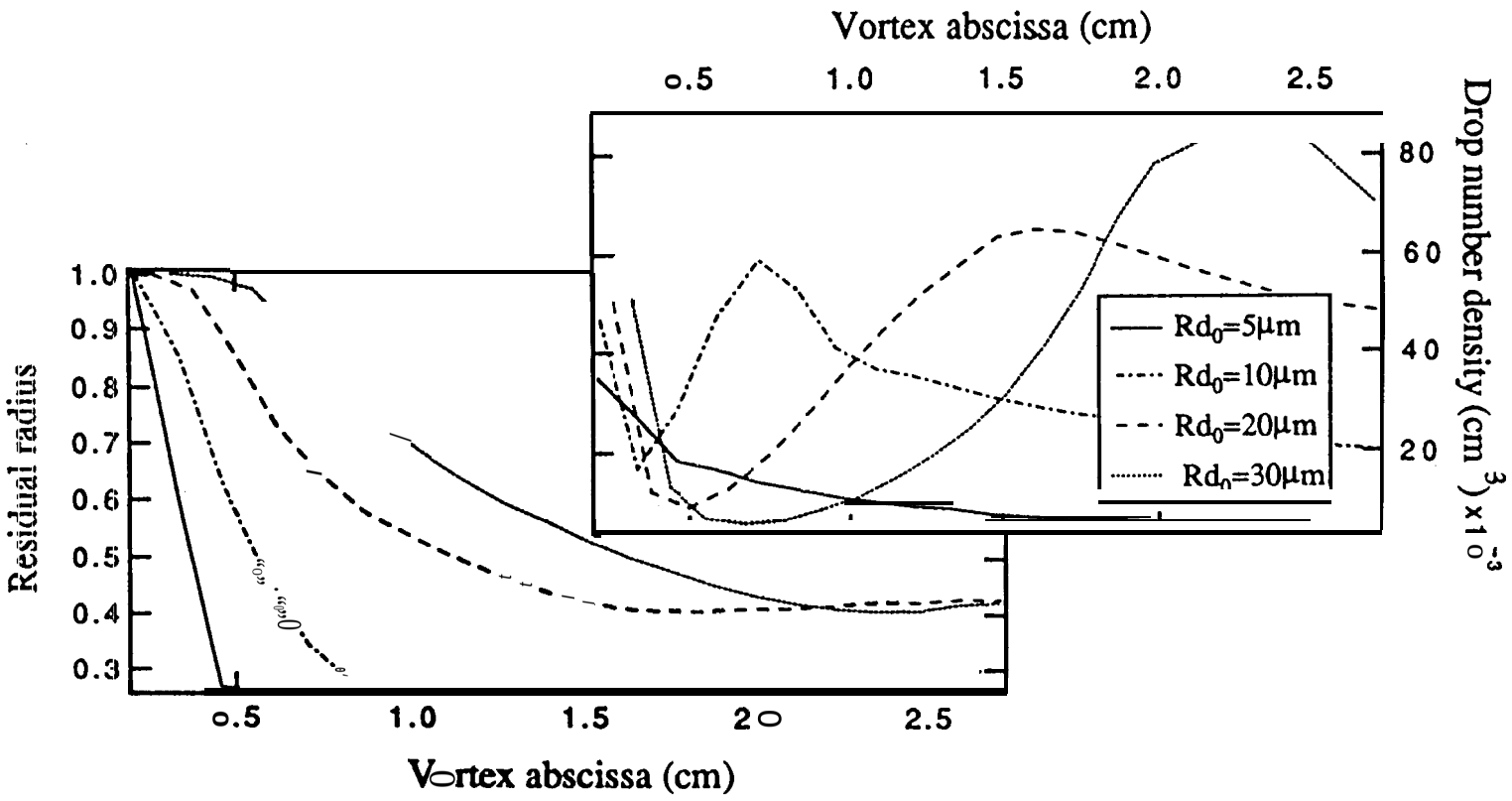
Vortex abscissa (cm)
0.5
1.0
1.5
2.0
2.5
Drop number density (cm^{-3}) x10^{-3}
80
60
40
20
Rd$_0$=5µm
Rd$_0$=10µm
Rd$_0$=20µm
Rd$_0$=30µm
Residual radius
1.0
0.9
0.8
0.7
0.6
0.5
0.4
0.3
0.5
1.0
1.5
2.0
2.5
Vortex abscissa (cm)

Fig 4

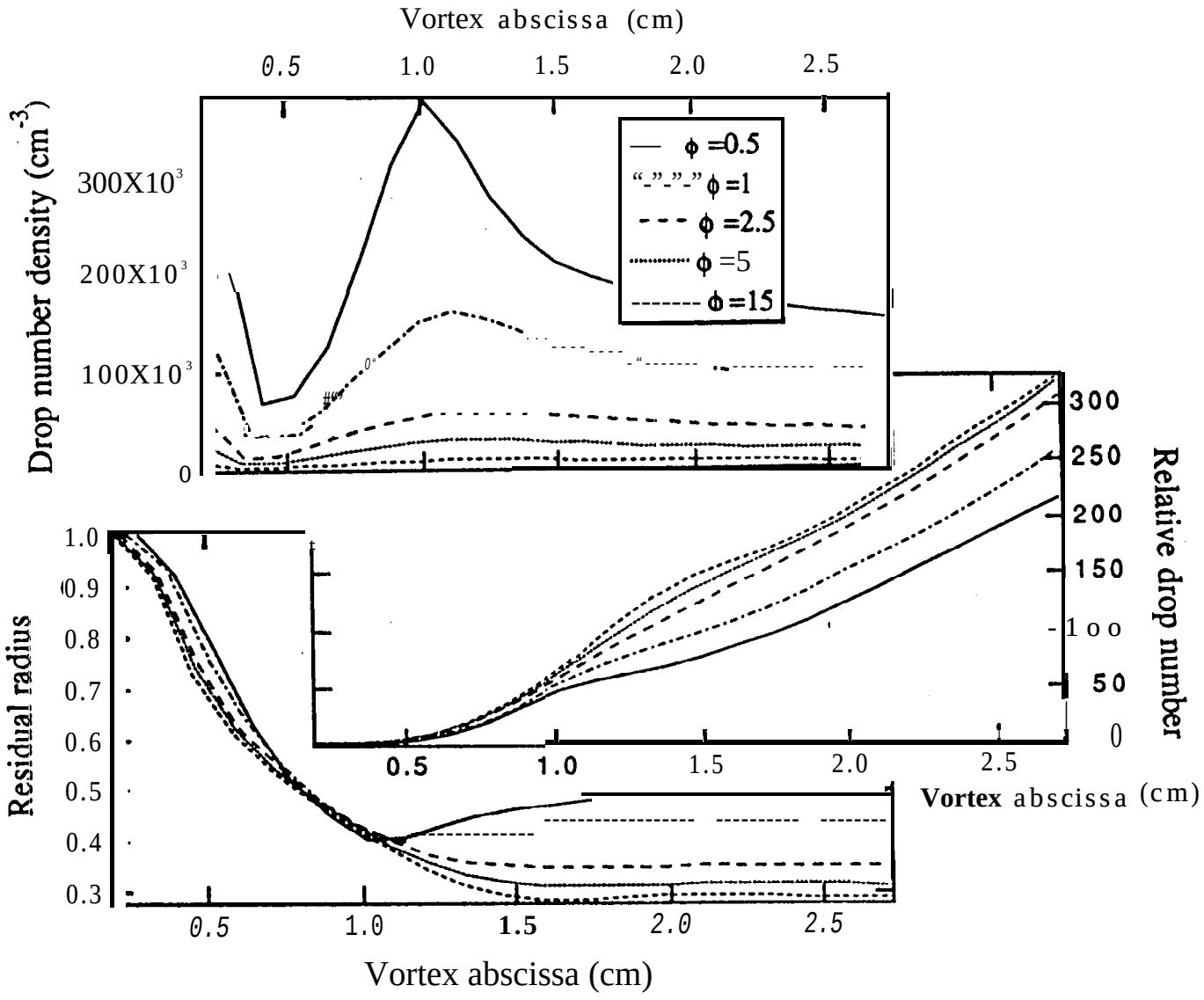
Vortex abscissa (cm)
0.5
1.0
1.5
2.0
2.5
Drop number density (cm-3)
300X10³
200X10³
100X10³
0
— ϕ =0.5
"-"-"-" ϕ =1
- - - ϕ =2.5
..... ϕ =5
------- ϕ =15
Relative drop number
300
250
200
150
100
50
0
Residual radius
1.0
0.9
0.8
0.7
0.6
0.5
0.4
0.3
Vortex abscissa (cm)
Vortex abscissa (cm)

Fig 5

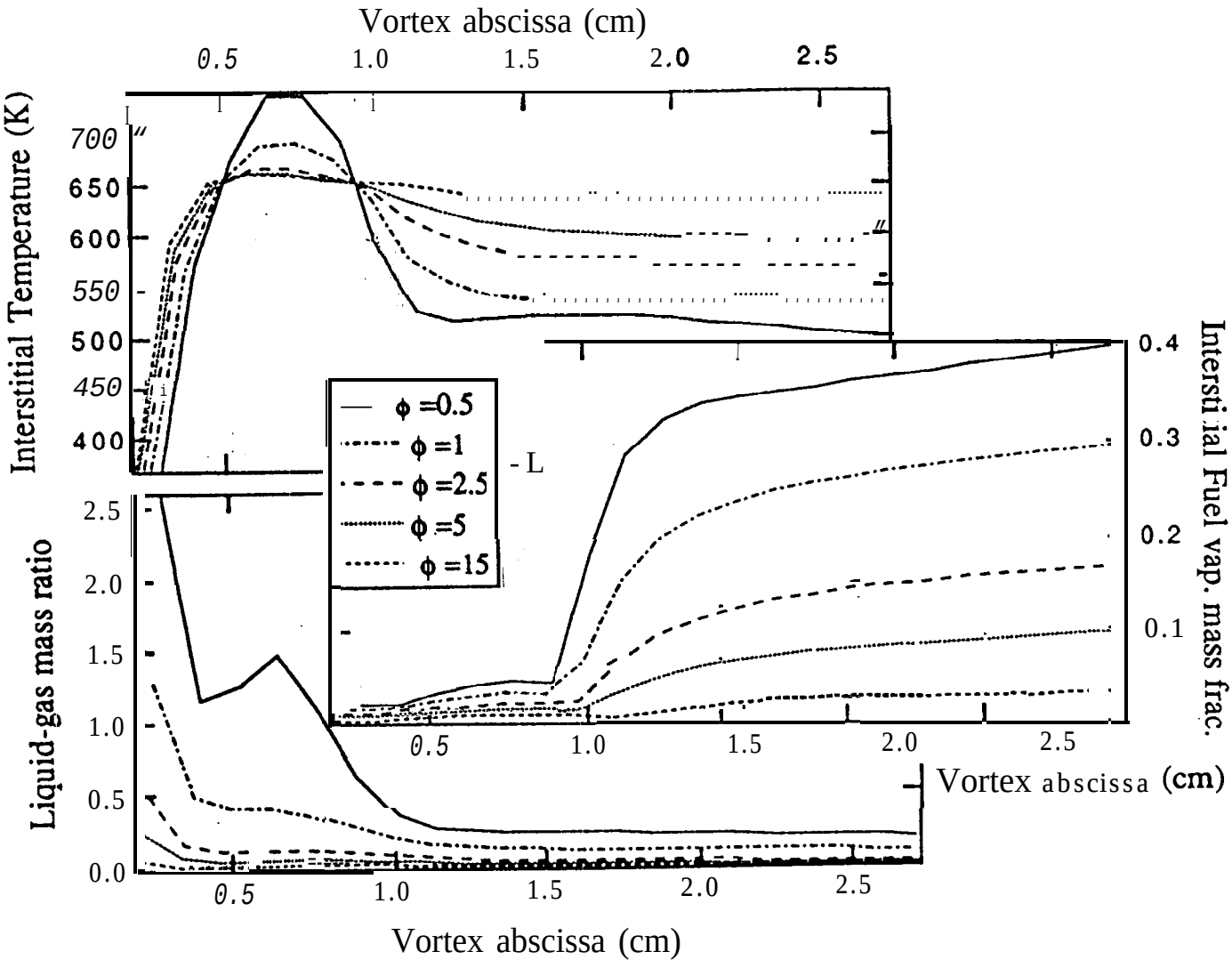
Vortex abscissa (cm)
0.5
1.0
1.5
2.0
2.5
Interstitial Temperature (K)
700
650
600
550
500
450
400
Liquid-gas mass ratio
2.5
2.0
1.5
1.0
0.5
0.0
Interstitial Fuel vap. mass frac.
0.4
0.3
0.2
0.1
ϕ =0.5
ϕ =1
ϕ =2.5
ϕ =5
ϕ =15
- L
Vortex abscissa (cm)

Fig c

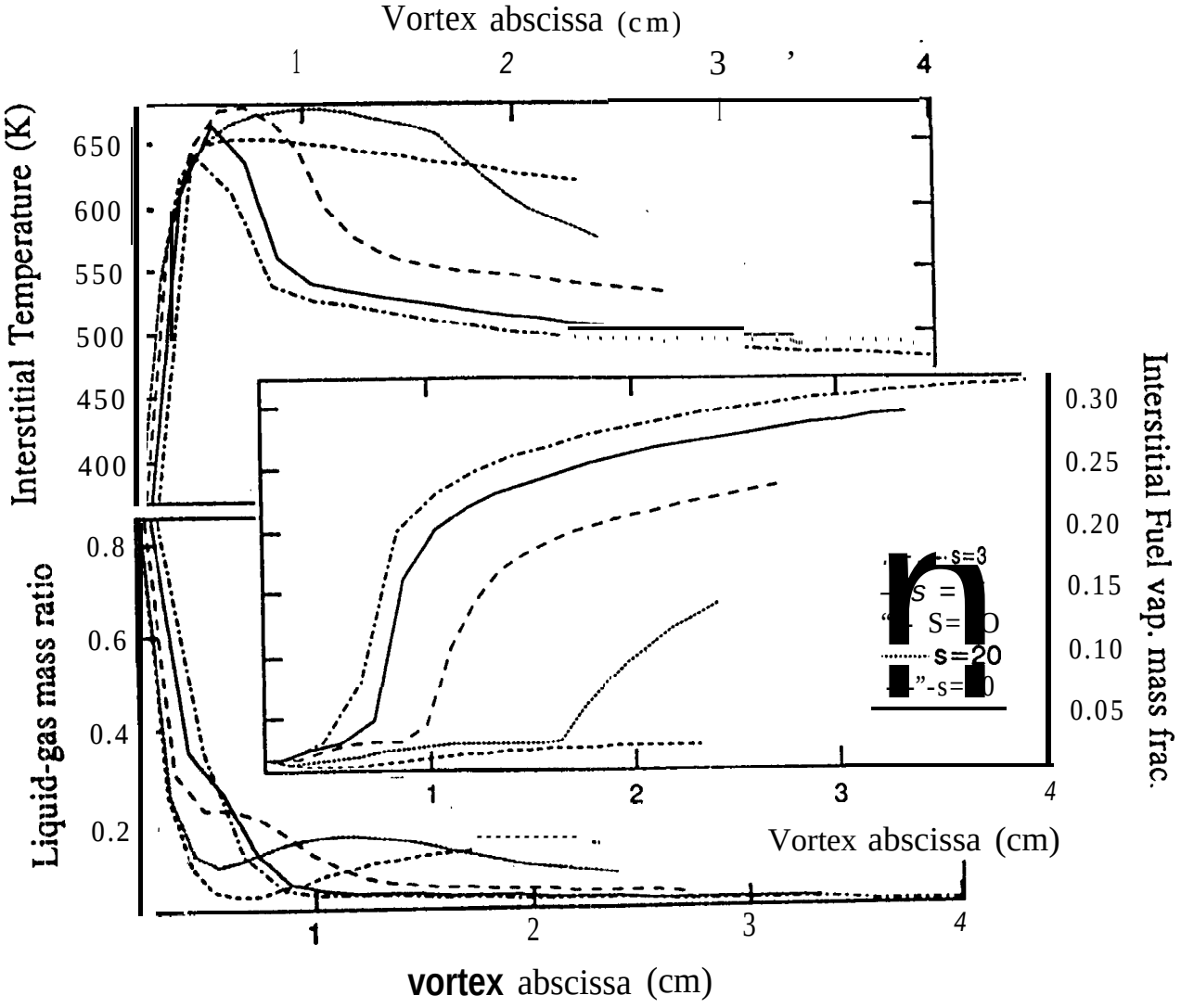
Vortex abscissa (cm)
1
2
3
4
Interstitial Temperature (K)
650
600
550
500
450
400
Liquid-gas mass ratio
0.8
0.6
0.4
0.2
Interstitial Fuel vap. mass frac.
0.30
0.25
0.20
0.15
0.10
0.05
s=3
s=20
Vortex abscissa (cm)
vortex abscissa (cm)

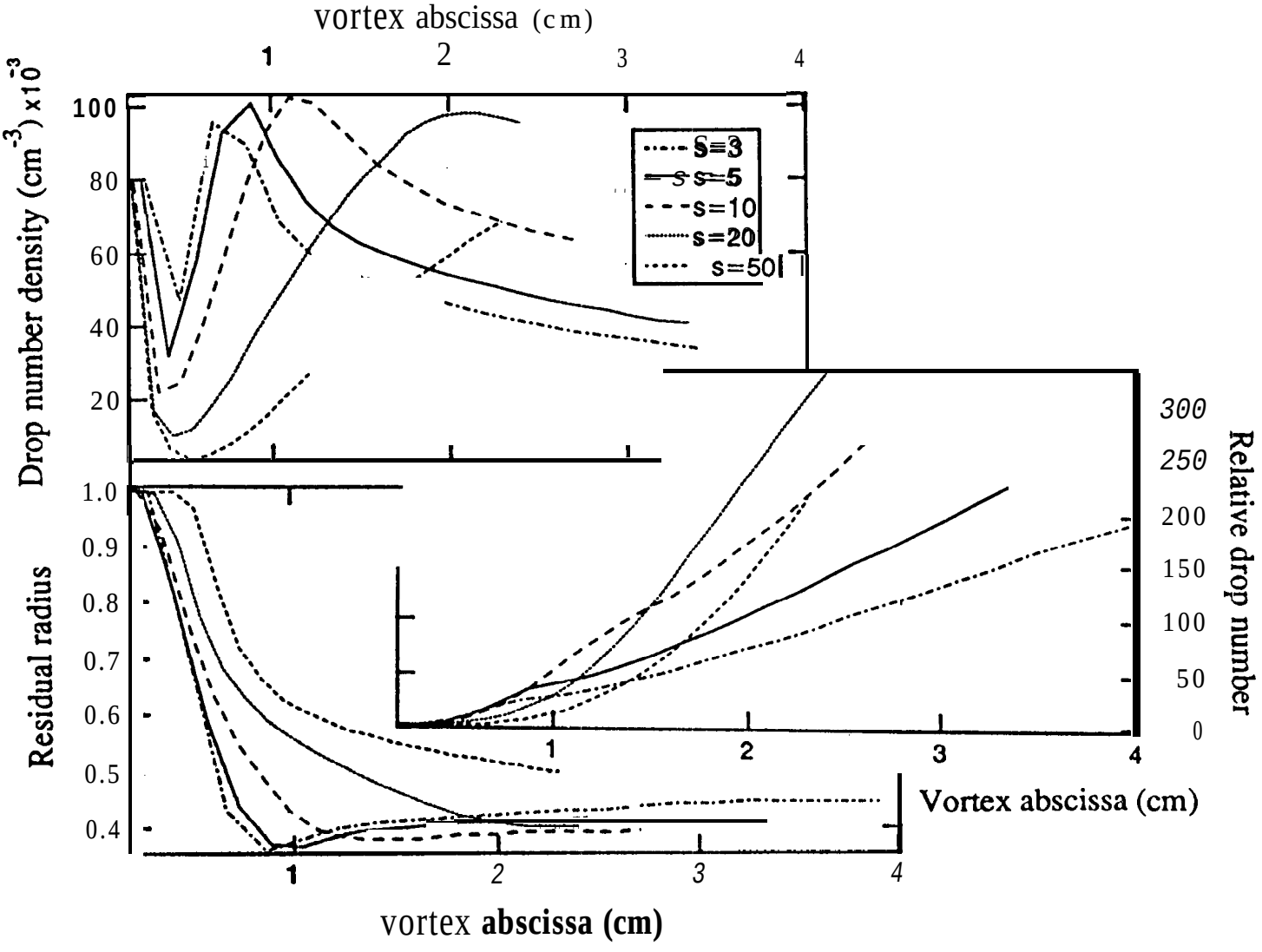
vortex abscissa (cm)
1
2
3
4
Drop number density (cm^{-3}) x10^{-3}
100
80
60
40
20
S=3
s=5
s=10
s=20
s=50
1.0
0.9
0.8
0.7
0.6
0.5
0.4
Residual radius
300
250
200
150
100
50
0
Relative drop number
Vortex abscissa (cm)
vortex abscissa (cm)